

# Physical controls on the storage of methane in landfast sea ice

J. Zhou<sup>1,2</sup>, J-L. Tison<sup>1</sup>, G. Carnat<sup>1</sup>, N-X. Geilfus<sup>3</sup> and B. Delille<sup>2,\*</sup>

[1]{Laboratoire de glaciologie, DSTE, Université Libre de Bruxelles, Brussels, Belgium}

[2]{Unité d'Océanographie chimique, MARE, Université de Liège, Liège, Belgium}

[3]{Arctic Research Center, Aarhus University, Aarhus, Denmark}

Correspondence to: J. Zhou (jiayzhou@ulb.ac.be)

## Abstract

We report on methane (CH<sub>4</sub>) dynamics in landfast sea ice, brine and under-ice seawater at Barrow in 2009. The CH<sub>4</sub> concentrations in under-ice water ranged between 25.9 and 116.4 nmol L<sup>-1</sup><sub>sw</sub>, indicating a supersaturation of 700 to 3100 % relative to the atmosphere. In comparison, the CH<sub>4</sub> concentrations in sea ice, ranged between 3.4 and 17.2 nmol L<sup>-1</sup><sub>ice</sub>, and the deduced CH<sub>4</sub> concentrations in brine, between 13.2 and 677.7 nmol L<sup>-1</sup><sub>brine</sub>. We investigated on the processes explaining the difference in CH<sub>4</sub> concentrations between sea ice, brine and the under-ice water, and suggest that biological controls on the storage of CH<sub>4</sub> in ice was minor in comparison to the physical controls. Two physical processes regulated the storage of CH<sub>4</sub> in our landfast ice samples: bubble formation within the ice and sea ice permeability. Gas bubble formation from solubility changes had favoured the accumulation of CH<sub>4</sub> in the ice at the beginning of ice growth. CH<sub>4</sub> retention in sea ice was then twice as efficient as that of salt; this also explains the overall higher CH<sub>4</sub> concentrations in brine than in the under-ice water. As sea ice thickened, gas bubble formation became less efficient, CH<sub>4</sub> was then mainly trapped in the dissolved state. The increase of sea ice permeability during ice melt marked the end of CH<sub>4</sub> storage.

## 1 **1 Introduction**

2 Methane (CH<sub>4</sub>) is a well-mixed greenhouse gas. Its concentration in the atmosphere is much  
3 lower than that of its oxidation product (CO<sub>2</sub>) (1.9 ppm *versus* 397 ppm respectively)  
4 (<http://www.esrl.noaa.gov/gmd/aggi/>). However, since CH<sub>4</sub> global warming potential is 28  
5 times higher than that of CO<sub>2</sub> over a 100-year frame, it accounts for 20 % of the global  
6 radiative forcing of the well-mixed greenhouse gases (Myhre et al., 2013).

7 Global ocean emission of CH<sub>4</sub> is estimated at 19 Tg per year (Kirschke et al., 2013), which is  
8 about 3 % of the global tropospheric CH<sub>4</sub> input. 75 % of that marine contribution is from  
9 coastal regions (Bange et al., 1994). CH<sub>4</sub> supersaturation relative to the atmosphere in  
10 estuaries (Borges and Abril, 2011; Upstill-Goddard et al., 2000) and coastal shelves  
11 (Kvenvolden et al., 1993; Savvichev et al., 2004; Shakhova et al., 2005; Shakhova et al.,  
12 2010) are indeed larger to that in the open ocean (Bates et al., 1996; Damm et al., 2010;  
13 Damm et al., 2008; Damm et al., 2007).

14 Methanogenesis in sub-marine sediments is thought to be the main process causing CH<sub>4</sub>  
15 efflux in the Arctic shelf regions. Nonetheless, other sources could also be significant: CH<sub>4</sub>  
16 seepage from coastal ice-complex deposits (Romanovskii et al., 2000) and from the deeper  
17 seabeds (Judd, 2004), and CH<sub>4</sub> dissociation in the shallow hydrates (Reagan and Moridis,  
18 2008; Westbrook et al., 2009). Recently, aerobic CH<sub>4</sub> production in the water column related  
19 to DMSP degradation was reported in the central Arctic (Damm et al., 2010), tropical  
20 upwelling areas (Florez-Leiva et al., 2013) and tropical oligotrophic areas (Zindler et al.,  
21 2012). However, the significance of that process over the Arctic shelf still needs to be  
22 assessed.

23 Ongoing global warming is likely to affect the various sources of CH<sub>4</sub> cited above, with  
24 positive feedback on the climate. Indeed, increase in sea temperature should increase  
25 methanogenic activities, leading to a more efficient conversion of organic matter to CH<sub>4</sub>  
26 (Zeikus and Winfrey, 1976). In addition, the induced seawater stratification is likely to change  
27 the nutrients ratio, which favours aerobic CH<sub>4</sub> production (Karl et al., 2008). Moreover,  
28 warmer seawater is likely to weaken the coastal ice-complex (including sub-sea permafrost)  
29 (Lawrence et al., 2008) and to displace the gas hydrate stability zones (Reagan and Moridis,  
30 2008), increasing gas seepage. Significant CH<sub>4</sub> escape has been recently detected via acoustic  
31 surveys along Spitsbergen continental margin (Westbrook et al., 2009), suggesting that

1 changes in the CH<sub>4</sub> storage system are ongoing. Since CH<sub>4</sub> has a high global warming  
2 potential, its release will enhance the global warming, which in turn will enhance  
3 methanogenic activities and gas seepages. This positive feedback contributed to rapid and  
4 significant climate warming in the past (O'Connor et al., 2010).

5 Understanding the current CH<sub>4</sub> budget is thus important to better simulate future climate  
6 scenarios. Many CH<sub>4</sub> measurements have been carried out in sediments and seawater  
7 throughout the coastal Arctic areas (Kvenvolden et al., 1993; Savvichev et al., 2004;  
8 Shakhova et al., 2005; Shakhova et al., 2010). These observations have led to speculations  
9 about potential CH<sub>4</sub> accumulation (Shakhova et al., 2010) and/or oxidation (Kitidis et al.,  
10 2010) under sea ice cover. Other studies further brought forward the role of sea ice in the  
11 exchange of CH<sub>4</sub> between seawater and the atmosphere (He et al., 2013; Kort et al., 2012).  
12 However, to the best of our knowledge, no study has yet discussed the physical controls on  
13 the storage of CH<sub>4</sub> in sea ice and its exchange at the atmosphere-ice-ocean interfaces. For  
14 instance, CH<sub>4</sub> mixing ratio up to 11 000 ppmV have been measured in sea ice bubbles  
15 (Shakhova et al., 2010), but the mechanisms leading to the incorporation of those gas bubbles  
16 within the ice have not been discussed. Similarly, He et al. (2013) suggested CH<sub>4</sub>  
17 consumption in the ice, based on their CH<sub>4</sub> fluxes above sea ice. However, they did not  
18 discuss the impact of sea ice permeability or ice melt on their results, while these parameters  
19 have been shown to affect other gas dynamics in sea ice (see e.g., Loose et al. (2009) for O<sub>2</sub>  
20 and SF<sub>6</sub>, Geilfus et al. (2012) and Nomura et al. (2010) for CO<sub>2</sub> and Zhou et al. (2013) for  
21 Ar). Therefore, we felt it necessary to highlight the physical controls on CH<sub>4</sub> dynamics in sea  
22 ice, from ice growth to ice melt. We have done this by investigating the annual evolution of  
23 CH<sub>4</sub> concentrations ([CH<sub>4</sub>]) in sea ice, in parallel with sea ice physical properties and [CH<sub>4</sub>] in  
24 seawater. To the best of our knowledge, we report here the first detailed time series of [CH<sub>4</sub>]  
25 in sea ice across seasons.

26

## 27 **2 Material and methods**

### 28 **2.1 Study site and physical framework**

29 Sea ice and under-ice seawater samples were collected during a field survey in the Chukchi  
30 Sea near Barrow (Alaska) (Fig. 1), from January through June 2009. The sampling was  
31 performed on level first-year landfast sea ice, within a square of 50 meters by 50 meters. The

1 north-eastern corner of the square was located at 71° 22.013' N, 156° 32.447' W. Seawater  
2 depth at the location was about 6.5 m  
3 ([http://seaice.alaska.edu/gi/observatories/barrow\\_sealevel](http://seaice.alaska.edu/gi/observatories/barrow_sealevel)). Ice cores were extracted and kept  
4 in the laboratory at -35 °C in the dark to prevent brine drainage and to limit biological  
5 activity. Temperature recorders indicated that the samples were always kept below -20 °C  
6 during the transport. All of the analyses were completed within the following year. A  
7 complete physical framework of the present study is presented and discussed in Zhou et al.  
8 (2013). We have selected 6 sampling events to illustrate the evolution of [CH<sub>4</sub>] at our  
9 location: one in the winter (BRW2; February 3), 4 in early spring (BRW4, BRW5, BRW6 and  
10 BRW7; corresponding to March 31, April 3, April 7 and April 10 respectively), and the final  
11 one in late spring (BRW10; June 5). The first 5 sampling events occurred during ice growth,  
12 the last one during ice decay.

## 13 **2.2 CH<sub>4</sub> in seawater**

14 [CH<sub>4</sub>] in seawater were determined by gas chromatography (GC) with flame ionization  
15 detection (SRI 8610C GC-FID) (Skoog et al., 1997), after creating a 30 mL headspace with  
16 N<sub>2</sub> in 70 mL glass serum bottles, following the procedure described by Abril and Iversen  
17 (2002). After creating the N<sub>2</sub> headspace, samples were vigorously shaken for 20 min and were  
18 placed in a thermostatic bath overnight at -1.6 °C. The following day, the samples were  
19 shaken again for 20 min before starting the GC analysis. CH<sub>4</sub>:CO<sub>2</sub>:N<sub>2</sub> mixtures (Air Liquide,  
20 Belgium) of 1, 10 and 30 ppm CH<sub>4</sub> were used as standards. The concentrations were then  
21 computed using the CH<sub>4</sub> solubility coefficient given by Yamamoto et al. (1976). The accuracy  
22 of the measurements was 1 %.

23 We calculated the solubility of CH<sub>4</sub> in seawater that is in equilibrium with the atmosphere,  
24 following Wiesenburg and Guinasso (1979). The ratio between the measured [CH<sub>4</sub>] in  
25 seawater and the calculated solubility in equilibrated seawater determines the supersaturation  
26 factor.

## 27 **2.3 CH<sub>4</sub> in bulk ice and brine**

28 We used the wet extraction method to extract CH<sub>4</sub> from sea ice, as described in Raynaud et al.  
29 (1982) for continental ice. Briefly, 80 g of ice sample were put in a small container, using a 5  
30 cm vertical resolution. The ice sample was then melted in the container under vacuum (10<sup>-3</sup>

1 torr), using a “bain-marie”. It was then slowly refrozen from the bottom, using an ethanol (96  
2 %) bath that was cooled to -80 °C by addition of liquid N<sub>2</sub>. After refreezing, the whole gas  
3 content (both dissolved and in the bubbles) was expelled to the headspace of the container.  
4 The expelled gas was then injected, through a 22 ml packed column (Mole Sieve 5 A 80/100;  
5 5 m x 1/8”), into a gas chromatograph (Trace GC) equipped with a flame ionisation detector  
6 for [CH<sub>4</sub>] measurement. The reproducibility of the measurement, based on triplicate analysis  
7 of 5 different standards, was 99.6%.

8 The method described here above gives [CH<sub>4</sub>] in bulk ice. Providing that there is no CH<sub>4</sub> in  
9 the pure ice matrix (Weeks, 2010), and hence that the entire amount of CH<sub>4</sub> (dissolved or in  
10 gas bubbles) is found within the ice pores (i.e. brine channels), [CH<sub>4</sub>] bulk ice divided by the  
11 brine volume fraction (Cox and Weeks, 1983) gives the deduced [CH<sub>4</sub>] in brine.

12 Dissolved [CH<sub>4</sub>] in brine was also measured on brine samples collected using the sackhole  
13 technique (e.g., Gleitz et al., 1995; Papadimitriou et al., 2007). Sackholes (partial core holes)  
14 were drilled at different depths, ranging from 20 to 130 cm. Brines, from adjacent brine  
15 channels and pockets, seeped into the sackholes and were collected after 10 to 60 min using a  
16 peristaltic pump (Cole Palmer, Masterflex® - Environmental Sampler). Each sackhole  
17 remained covered with a plastic lid to minimize mixing with the free-atmosphere. Brines were  
18 collected in 70 mL glass serum bottles, filled to overflowing, poisoned with 100 µL of  
19 saturated HgCl<sub>2</sub> and sealed with butyl stoppers and aluminium caps. The measured [CH<sub>4</sub>] in  
20 brine is an integrated value of the CH<sub>4</sub> in brine from all the ice layers above the sampling  
21 depth. Therefore, the vertical resolution is lower than that of the [CH<sub>4</sub>] in brine that is  
22 deduced from the [CH<sub>4</sub>] in bulk ice. It is also noteworthy that the relative contribution of the  
23 various depth levels is unknown and dependent on the brine volume changes with depth.  
24 However, it is of interest to compare the measured [CH<sub>4</sub>] in brine with the [CH<sub>4</sub>] in brine that  
25 is deduced from the bulk ice values, as discussed later on.

26 For data interpretation, we calculated CH<sub>4</sub> solubility in brine and in ice (i.e., potential [CH<sub>4</sub>]  
27 dissolved in brine and in bulk ice respectively). The solubility of CH<sub>4</sub> in brine was calculated  
28 using the temperature and salinity-dependent solubility of Wiesenburg and Guinasso (1979)  
29 as for seawater. This is allowed providing that the relationship of Wiesenburg and Guinasso  
30 (1979) is valid for the ranges of brine-temperature and -salinity. As for the conversion of  
31 [CH<sub>4</sub>] in bulk ice into the deduced [CH<sub>4</sub>] in brine, we simply multiplied the solubility of CH<sub>4</sub>  
32 in brine by the brine volume fraction to get the solubility of CH<sub>4</sub> in bulk ice. Brine salinity

1 and brine volume (used in the calculations) were derived from the relationship of Cox and  
2 Weeks (1983). The ratio between the observed  $[\text{CH}_4]$  in ice or brine to their respective  
3 calculated solubility determines the supersaturation factor.

4 In addition, we computed the standing stock of  $\text{CH}_4$ , i.e., the total amount of  $\text{CH}_4$  within the  
5 ice cover. To do so, we integrated the concentrations of  $\text{CH}_4$  in bulk ice vertically to obtain  
6 the  $\text{CH}_4$  content per square meter of ice.

7 For further comparison with the literature, we also computed  $\text{CH}_4$  mixing ratios. It is usually  
8 obtained by dividing the number of moles of  $\text{CH}_4$  by the total gas content. However, since we  
9 did not measure the total gas content, we used instead the sum of measured atmospheric-  
10 dominant gases ( $\text{O}_2$ ,  $\text{N}_2$  and Ar, data not shown).

11

## 12 **3 Results**

### 13 **3.1 $\text{CH}_4$ concentration in ice**

14  $[\text{CH}_4]$  in bulk ice ranged between  $3.4 \text{ nmol L}_{\text{ice}}^{-1}$  and  $17.2 \text{ nmol L}_{\text{ice}}^{-1}$ . Mean  $[\text{CH}_4]$  increased  
15 from BRW2 ( $6.4 \text{ nmol L}_{\text{ice}}^{-1}$ ) to BRW7 ( $7.8 \text{ nmol L}_{\text{ice}}^{-1}$ ) and decreased to  $5.5 \text{ nmol L}_{\text{ice}}^{-1}$  at  
16 BRW10. This evolution parallels that of the standing stocks of  $[\text{CH}_4]$  which increased from  
17 BRW2 ( $5070$  to  $5430 \text{ nmol m}^{-2}$ ) to BRW7 ( $9200 \text{ nmol m}^{-2}$ ), then decreased at BRW10 ( $7580$   
18  $\text{nmol m}^{-2}$ ) (Fig. 2). For data interpretation, sea ice thickness is also shown in Fig. 2. It appears  
19 that the mean  $[\text{CH}_4]$  and the standing stock increased as sea ice thickened from BRW2 to  
20 BRW7, but decreased at BRW10 despite the fact that sea ice was thicker there.

21 The individual profiles of  $[\text{CH}_4]$  in bulk ice (Fig. 3a) for each sampling event further highlight  
22 the contrasts between BRW10 and all the previous sampling events (BRW2 to BRW7): all the  
23  $[\text{CH}_4]$  profiles in ice from BRW2 to BRW 7 can be divided into 3 main zones. The first one  
24 ranged from 0 to 25 cm, where a peak of  $[\text{CH}_4]$  was found at 15 to 25 cm.  $[\text{CH}_4]$   
25 measurements made on a twin ice core of BRW2 (duplicate) show that spatial variability in  
26 the layer of 15 to 25 cm could reach 60 %. The second zone was found in the ice interior, and  
27 ranged from 25 cm to the upper limit of the permeable layers (shaded area), where  $[\text{CH}_4]$  were  
28 close to  $5 \text{ nmol L}_{\text{ice}}^{-1}$ . The third zone corresponds to the permeable layers where  $[\text{CH}_4]$   
29 increased again toward the sea ice bottom, with values ranging between 5 to  $10 \text{ nmol L}_{\text{ice}}^{-1}$ . At  
30 BRW10, as the whole ice cover became permeable (shaded area at all depths), the whole

1 profile flattened: the peak of [CH<sub>4</sub>] around 15 to 25 cm disappeared, the ice interior still has a  
2 baseline at 5 nmol L<sub>ice</sub><sup>-1</sup> and the increase of [CH<sub>4</sub>] at the bottom was less obvious than in the  
3 previous sampling events.

4 Beside the strong vertical variation, [CH<sub>4</sub>] in bulk ice were always higher than the solubility  
5 values in surface seawater that would have been in equilibrium with the atmosphere (3.8 nmol  
6 L<sub>sw</sub><sup>-1</sup>) and the theoretical solubility in ice at all depths (Fig. 3a – white dots). [CH<sub>4</sub>] in bulk ice  
7 were in average 1.8 times higher than that in surface seawater and 75 times higher than the  
8 theoretical solubility in ice. The highest supersaturation factor reached 396 and was measured  
9 in BRW6, at 20 to 25 cm depth. Again, BRW10 differed from all the other sampling events,  
10 with lower supersaturation factor (mean supersaturation and standard deviation were 11+/-4  
11 versus 86+/-68 for BRW2 to BRW7).

12 CH<sub>4</sub> mixing ratio (not shown) was also measured for BRW2, BRW4, BRW7 and BRW10. It  
13 ranged between 5.8 and 105.3 ppmV. The maximum mixing ratio was found in BRW4, at 15  
14 to 20 cm depth; this is 3.6 times higher than the mean mixing ratio of 29 ppmV.

15 To summarize, BRW10 differed from all the other samplings events by its lower mean [CH<sub>4</sub>]  
16 and its flatter [CH<sub>4</sub>] profiles. Although all the ice samples were supersaturated relative to the  
17 ice and surface seawater, larger supersaturations were observed from BRW2 to BRW7 (less  
18 permeable ice cores) compared to BRW10 (entirely permeable ice core), especially at 15 to 25  
19 cm depth where both [CH<sub>4</sub>] and CH<sub>4</sub> mixing ratio were found to be the highest.

## 20 **3.2 CH<sub>4</sub> concentration in brine**

21 Deduced [CH<sub>4</sub>] in brine (using [CH<sub>4</sub>] in ice) ranged between 13.2 nmol L<sub>brine</sub><sup>-1</sup> and 677.7  
22 nmol L<sub>brine</sub><sup>-1</sup>. These are thus much higher than the range of [CH<sub>4</sub>] measured in brine sackholes  
23 (10.0 to 36.2 nmol L<sub>brine</sub><sup>-1</sup>) (Fig. 3– triangles) and in seawater (25.9 and 116.4 nmol L<sub>sw</sub><sup>-1</sup>).

24 The evolution of [CH<sub>4</sub>] in brine across seasons was rather similar to that of [CH<sub>4</sub>] in bulk ice,  
25 except in the bottom layers. Indeed, from BRW2 to BRW7, high [CH<sub>4</sub>] in brine were also  
26 observed at 15 to 20-cm depth; but from that level, [CH<sub>4</sub>] in brine decreased and reached the  
27 lowest values at the sea ice bottom, where it is similar to observed CH<sub>4</sub> values in seawater.  
28 There was thus no slight increase of [CH<sub>4</sub>] in brine, as observed in the [CH<sub>4</sub>] in bulk ice, at  
29 the sea ice bottom. The profile of [CH<sub>4</sub>] in brine flattened at BRW10, with values ranging  
30 between 13.2 and 87.0 nmol L<sub>brine</sub><sup>-1</sup>, which were less variable and much closer to both the  
31 solubility values in brine and the actual measured [CH<sub>4</sub>] in brine than the ranges of values in

1 the previous sampling events ( $35.6 \text{ nmol L}_{\text{brine}}^{-1}$  and  $677.7 \text{ nmol L}_{\text{brine}}^{-1}$ ). The minimum of  
2  $[\text{CH}_4]$  in brine was calculated at 12.5 cm. Temperature data was missing at the very surface,  
3 so that we could not compute  $[\text{CH}_4]$  in brine above 12.5 cm.

### 4 **3.3 CH<sub>4</sub> concentration in seawater**

5 Measured  $[\text{CH}_4]$  in seawater ranged between 25.9 and  $116.4 \text{ nmol L}_{\text{sw}}^{-1}$  (Fig. 3c). This is 7 to  
6 31 times higher than seawater in equilibrium with the atmosphere ( $3.8 \text{ nmol L}^{-1}$  for a salinity  
7 of 35 at  $0^\circ\text{C}$ ) (Wiesenburg and Guinasso, 1979).

8 Measurements of  $[\text{CH}_4]$  in seawater were homogenous in time from BRW2 to BRW7, with a  
9 mean value and standard deviation of  $42.0 \pm 2.4 \text{ nmol L}_{\text{sw}}^{-1}$  for BRW2 and  $37.5 \pm 6 \text{ nmol}$   
10  $\text{L}_{\text{sw}}^{-1}$  for BRW 4 to BRW7. They then increased at all depths, at BRW10 and reached a mean  
11 value and standard deviation of  $77.4 \pm 27.8 \text{ nmol L}_{\text{sw}}^{-1}$ .

12

## 13 **4 Discussion**

14 The present paper aims at understanding the physical controls on the  $[\text{CH}_4]$  in sea ice.  
15 Discussing the physical controls only makes sense if the variations of  $[\text{CH}_4]$  due to biological  
16 activity are negligible compared to those due to physical processes. Therefore, we will first  
17 assess the importance of biological activity on the variation of  $[\text{CH}_4]$  (Sect. 4.1), before  
18 discussing the physical controls on the profiles of  $[\text{CH}_4]$  in sea ice and brine (Sect. 4.2).

### 19 **4.1 Impact of biological activity on $[\text{CH}_4]$**

20 To assess the impact of biological activity on  $[\text{CH}_4]$ , we recalculated the standing stocks of  
21 BRW4 to BRW7 (Fig. 3), by considering every 5-cm ice sample in the 25 to 80 cm-depth  
22 layers. These choices are motivated by the following reasons: First, we suggest focusing on  
23 the standing stocks of the impermeable layers (i.e. layers that have a brine volume fraction  
24 below 5 % (Golden et al., 1998); layers above the shaded areas on Fig. 3a, b). These layers  
25 are considered as a closed system in terms of brine dynamics and are therefore suitable to  
26 assess biological transformation of  $\text{CH}_4$ . Second, we felt it appropriate to ignore the upper  
27 layer (0 to 25 cm), since spatial variability could be important in these layers (up to 60 %  
28 from 15 to 25 cm depth) as shown in Figure 3a – BRW2. Third, we only focused on the



1 sampling events that were collected at short time intervals (3 or 4 days), i.e., BRW4 to  
2 BRW7, rather than between BRW2 and BRW4 (56 days). This is mainly due to the similar  
3 physical properties of the ice cores collected at short-time-intervals (i.e., in terms of ice core  
4 length, ice temperature, ice salinity profiles).

5 Deduced CH<sub>4</sub> standing stocks in the 5-cm ice samples (in the 25 to 80-cm ice layers, from  
6 BRW4 to BRW7) varied between 198 and 375 nmol m<sup>-2</sup>, with a mean and standard deviation  
7 of 271 +/- 41 nmol m<sup>-2</sup>. We performed an ANOVA test on these standing stocks (n=44) and  
8 differences between the samplings were not significant enough to exclude the possibility of  
9 random sampling variability.

10 In addition, we plotted chlorophyll-a concentrations against [CH<sub>4</sub>] in bulk ice, and phosphate  
11 concentrations against [CH<sub>4</sub>] in bulk ice, to investigate on potential in situ production of CH<sub>4</sub>  
12 in both permeable and impermeable ice layers (see Appendix A). The rationale is that  
13 previous studies have shown strong correlation between these variables (Damm et al., 2008;  
14 Damm et al., 2010) where CH<sub>4</sub> production was found to occur. As there is no obvious  
15 correlation between the presented variables (see Appendix A), we surmise that the pathway of  
16 CH<sub>4</sub> production that was observed in Damm et al., 2008; 2010 may not have occurred in the  
17 present study.

18 Furthermore, the turnover time for CH<sub>4</sub> oxidation in the Arctic Ocean exceeds 1.5 years  
19 (Griffiths et al. 1982 and Valentine et al. 2001), which is much longer than the lifetime of first  
20 year landfast ice. If we assume that the turnover time is similar in landfast sea ice, then we do  
21 not expect to find major CH<sub>4</sub> oxidation in our ice samples.

22 Because CH<sub>4</sub> production is unlikely in sea ice and CH<sub>4</sub> oxidation may be slow, we conclude  
23 that biological transformation of CH<sub>4</sub> is negligible in comparison with the amount of CH<sub>4</sub> that  
24 was physically incorporated in the impermeable ice layers, which is consistent with the  
25 findings derived from the standing stocks. Therefore, the discussion below will mainly focus  
26 on the physical processes that regulate CH<sub>4</sub> concentrations in sea ice.

## 1 **4.2 The mechanisms for CH<sub>4</sub> incorporation, enrichment and dilution in sea ice**

### 2 **4.2.1 Range of CH<sub>4</sub> in sea ice and seawater, comparison with the** 3 **literature**

4 Our [CH<sub>4</sub>] in sea ice (3.4 - 17.2 nmol L<sub>ice</sub><sup>-1</sup>) were slightly lower than those of Lorenson and  
5 Kvenvolden (1995) (15 nmol L<sub>ice</sub><sup>-1</sup> to 40 nmol L<sub>ice</sub><sup>-1</sup>). The deduced mixing ratios (5.8 ppmV  
6 to 105.3 ppmV) were however much lower than the 11 000 ppmV of Shakhova et al. (2010).  
7 We attribute the observed differences to (1) [CH<sub>4</sub>] in seawater and (2) ebullition processes  
8 (i.e., the seepage of CH<sub>4</sub> bubbles from the seafloor and their rising through the water column).

9 First, our [CH<sub>4</sub>] in seawater (25.9 and 116.4 nmol L<sub>sw</sub><sup>-1</sup>) are consistent with those reported in  
10 northern Alaska (10.7 nmol L<sub>sw</sub><sup>-1</sup> to 111.8 nmol L<sub>sw</sub><sup>-1</sup> (Kvenvolden et al., 1993)) and shallow  
11 shelf areas with CH<sub>4</sub> release from sediment and/or destabilized gas hydrate (2.1 nmol L<sub>sw</sub><sup>-1</sup> to  
12 154 nmol L<sub>sw</sub><sup>-1</sup> (Shakhova et al., 2005)), but are much lower than the measurements reported  
13 by Shakhova et al. (2010) (1.8 to 2880 nmol L<sub>sw</sub><sup>-1</sup>). The differences in [CH<sub>4</sub>] in seawater lead  
14 to contrasting CH<sub>4</sub> supersaturations (700 % and 3100 % in the present study versus 100 % to  
15 160 000% in Shakhova et al. (2010)). Assuming similar incorporation rates in both studies,  
16 lower CH<sub>4</sub> supersaturation in seawater leads to lower CH<sub>4</sub> incorporated into sea ice and hence  
17 lower CH<sub>4</sub> mixing ratio in sea ice.

18 Second, ebullition is a process associated with rapid bubble ascension, limiting gas  
19 equilibration with the surrounding water mass (Keller and Stallard, 1994). Therefore, in  
20 shallow locations, CH<sub>4</sub> bubbles released from the seafloor could reach the seawater surface  
21 (Keller and Stallard, 1994; McGinnis et al., 2006). We believe that ebullition could increase  
22 CH<sub>4</sub> at the sea ice-water interface and lead to larger CH<sub>4</sub> incorporation into sea ice than if the  
23 ebullition was absent. Ebullitions were clearly observed in the Siberian Arctic Shelf  
24 (Shakhova et al., 2010) and in that case, centimetre-size bubbles were found within the ice  
25 (Shakhova et al., 2010). Since we did not find any literature reporting ebullition processes at  
26 Barrow, and since our ice cores generally showed millimeter-size bubbles (Zhou et al., 2013),  
27 we believe that ebullition processes were much less important in our study than in Shakhova  
28 et al. (2010).

## 4.2.2 Mechanisms responsible for the evolution of the vertical profiles of [CH<sub>4</sub>] in bulk ice and brine during ice growth

Although the CH<sub>4</sub> source was seawater, [CH<sub>4</sub>] in bulk ice from BRW2 to BRW7 did not show a C-shape profile, as would salinity for growing sea ice (Petrich and Eicken, 2010). For instance, instead of a surface maximum for salt, we observed a sub-surface maximum for CH<sub>4</sub>. As discussed below, we propose three abiotic mechanisms to explain the salient features of the [CH<sub>4</sub>] vertical profiles in Barrow bulk ice: (1) gas escape during the initial ice growth phase in the surface layer (2) preferential gas accumulation in the sub-surface and (3) brine volume fraction effect for the bottom layer.

We assume that CH<sub>4</sub>, similarly to CO<sub>2</sub>, could escape from the ice to the atmosphere, at the beginning of the ice growth (Geilfus et al., 2013; Nomura et al., 2006) (Fig. 4). In addition, once sea ice is consolidated, changes in temperature and in the volume of brine pockets are likely to fracture the ice, causing the expulsion of brines (Notz and Worster, 2009) and air bubbles (Untersteiner, 1968) at the ice surface. These 2 processes could explain the decrease of [CH<sub>4</sub>] in bulk ice at the very surface of sea ice (Fig. 3).

Preferential gas accumulation during ice growth has been described for argon (Ar) in Zhou et al. (2013): Temperature and salinity changes in brine at sea ice formation lead to a sharp decrease of CH<sub>4</sub> solubility that favours bubble nucleation in sea ice. Once formed, the bubbles migrate upward due to their buoyancy. They are blocked under the surface impermeable layer, leading to gas accumulation (Fig. 4). Such process is supported by 2 characteristics: the presence of bubbles and the occurrence of large supersaturation levels (compared to the rest of the ice core). The presence of bubbles was observed on thin sections by Zhou et al. (2013) and is also coherent with the large difference between the deduced CH<sub>4</sub> in brine (which includes both CH<sub>4</sub> in bubbles and CH<sub>4</sub> that is dissolved in brine) (Fig. 3b, squares) and the actual measurements of CH<sub>4</sub> in brine (only CH<sub>4</sub> that is dissolved in brine) (Fig. 3, triangles). Moreover, the largest CH<sub>4</sub> supersaturations relative to CH<sub>4</sub> solubility in ice were always found at 15 cm to 25 cm depth, which correspond to the ice depth were Zhou et al. (2013) have observed bubble accumulation and Ar supersaturation up to 2900 %. Therefore, the mechanism of preferential gas accumulation suggested for Ar may be relevant for CH<sub>4</sub> as well. Larger CH<sub>4</sub> supersaturation as compared to Ar supersaturation is likely due to the difference in CH<sub>4</sub> and Ar solubility; CH<sub>4</sub>, which is less soluble than Ar, would be more affected by temperature and salinity changes. It is also noteworthy that this process of bubble

1 formation in sea ice led to large spatial variability as witnessed by the duplicate of BRW2,  
2 which showed up to 60% of CH<sub>4</sub> variation at 15 – 25 cm depth.

3 As the freezing front progresses, the temperature gradient in the permeable layer reduces;  
4 bubble nucleation from solubility decrease is less efficient. As a consequence, CH<sub>4</sub>  
5 accumulates less and [CH<sub>4</sub>] in brine decreases towards the bottom. Such a decrease is  
6 however not observed for [CH<sub>4</sub>] in bulk ice. We attribute this to the brine volume fraction  
7 effect: a larger brine volume may contain a larger amount of CH<sub>4</sub> molecules, which induces  
8 higher CH<sub>4</sub> concentrations in bulk ice. The fact that CH<sub>4</sub> in brine did not show the increase at  
9 the bottom of the ice supports this suggestion.

10 An alternative explanation to the preferential gas accumulation due to solubility changes  
11 would be that of a direct bubble incorporation after a sudden but intense release of CH<sub>4</sub>  
12 bubbles from the sediment to the ice bottom. CH<sub>4</sub> release from sediment is possible since our  
13 [CH<sub>4</sub>] in seawater are consistent with that found in areas where CH<sub>4</sub> release from sediment  
14 and/or gas hydrate destabilization likely occur (see section 4.2.1). However, this process does  
15 not explain the slow decrease of [CH<sub>4</sub>] in brine from 15 – 25 cm depth to the sea ice bottom  
16 (Fig. 3b), and we may also wonder why the ebullition only occurred once during the whole  
17 sampling period.

18 The contribution of in situ bubble formation in the retention of CH<sub>4</sub> in sea ice is assessed in  
19 Fig. 5. We calculated the ratio between CH<sub>4</sub> in ice and the CH<sub>4</sub> in seawater at BRW2 (44  
20 nmol L<sup>-1</sup><sub>sw</sub>), and the ratio between brine salinity and the salinity of seawater at BRW2 (32), at  
21 each ice depth, for all the sampling events. The CH<sub>4</sub> in seawater and the salinity of seawater  
22 of BRW2 were chosen as references for consistency with Zhou et al. (2013). Similar apparent  
23 fractionation means that CH<sub>4</sub> is retained (incorporated and transported) in sea ice in the same  
24 way to salt, while a difference in the apparent fractionation means a difference in their  
25 retention processes.

26 Four main observations can be made on Fig. 5. First, the apparent fractionation averaged 15  
27 % but never reached 100 %. This is due to the rejection of impurities during sea ice formation  
28 (Weeks, 2010). Our study therefore suggests that sea ice rejects about 85 % of its impurities,  
29 but retains 15 % of them. This is in agreement with Petrich and Eicken (2010) suggesting that  
30 sea ice brine allows a retention of 10 to 40 % of seawater ions in the ice. Second, the highest  
31 apparent fractionation of CH<sub>4</sub> (up to 39 %) was observed at 15 to 25 cm-depth; in that layer,  
32 the retention of CH<sub>4</sub> could be higher than that of salt by a factor of 2. This supports the

1 previous suggestion about preferential gas accumulation: the presence of gas bubbles allows  
2 higher retention of CH<sub>4</sub> than salt. Third, the apparent fractionation of CH<sub>4</sub> was lower than that  
3 of salt at the surface of all the sampling events, except at BRW10. We believe that these are  
4 related to the large permeability of the ice during its formation and/or the formation of some  
5 cracks at the ice surface (during the cold period), which have allowed gas to escape from sea  
6 ice to the atmosphere, as explained earlier in this section. The lower [CH<sub>4</sub>] in bulk ice at these  
7 sampling events (Fig. 3a) tends to support the conjecture of gas escape. Four, below the top  
8 layer of about 25 cm of ice, both CH<sub>4</sub> and salt enrichment values are similar, indicating that in  
9 these ice layers, CH<sub>4</sub> was mainly incorporated in the dissolved state, as salt was.

#### 10 **4.2.3 Sea ice permeability controls [CH<sub>4</sub>] in bulk ice and brine during sea** 11 **ice decay**

12 At BRW10, both [CH<sub>4</sub>] in bulk ice and deduced [CH<sub>4</sub>] in brine decreased and became less  
13 variable than the previous samplings (BRW2 to BRW7). In addition, CH<sub>4</sub> standing stocks  
14 decreased by ca. 1600 nmol m<sup>-2</sup> from BRW7 to BW10, and the deduced [CH<sub>4</sub>] in brine  
15 became closer to the measured [CH<sub>4</sub>] in brine. These measurements suggest an enhanced gas  
16 transport through the ice and that gas bubbles have escaped from sea ice to the atmosphere.  
17 Gas escape was allowed given that sea ice was permeable at all depths (Fig. 3a, b – shaded  
18 area). Concomitant Ar bubble escape was suggested in Zhou et al. (2013). However, in  
19 contrast to Ar that was then at saturation, CH<sub>4</sub> was still supersaturated compared to the  
20 solubility in brine. This could be related to a slow exchange between the atmosphere, brine  
21 and the supersaturated seawater through diffusion.

22 [CH<sub>4</sub>] in brine at BRW10 (13.2 nmol L<sub>brine</sub><sup>-1</sup> to 87.0 nmol L<sub>brine</sub><sup>-1</sup>) ranged between [CH<sub>4</sub>] at  
23 ice/water interface (116.4 nmol L<sub>sw</sub><sup>-1</sup>) and the theoretical [CH<sub>4</sub>] in surface seawater that is in  
24 equilibrium with the atmosphere (3.8 nmol L<sub>sw</sub><sup>-1</sup>). Although [CH<sub>4</sub>] in brine at the very surface  
25 (0 – 12.5 cm) could not be retrieved, we can hypothesize that the gradient of [CH<sub>4</sub>] between  
26 the ice/seawater interface and the ice surface led to CH<sub>4</sub> diffusion from ice/seawater interface  
27 to the ice surface, and therefore maintained [CH<sub>4</sub>] supersaturated in ice, after gas bubble  
28 escape. Since the source of [CH<sub>4</sub>] was from supersaturated seawater, [CH<sub>4</sub>] in brine was  
29 slightly higher at the sea ice bottom than at the top.

30

## 1 **5 Conclusions and perspectives**

2 We reported on [CH<sub>4</sub>] evolution in landfast sea ice and in under-ice water from February  
3 through June 2009 at Barrow (Alaska). Our [CH<sub>4</sub>] in sea ice and [CH<sub>4</sub>] in seawater are  
4 consistent with records from the area with CH<sub>4</sub> release from sediment and gas hydrate  
5 destabilization (Kvenvolden et al., 1993; Lorenson and Kvenvolden, 1995; Shakhova et al.,  
6 2010).

7 As summarized in Fig. 4, gas exchange likely took place during initial ice growth between sea  
8 ice and the atmosphere, and the formation of cracks could also lead to a decrease of CH<sub>4</sub> at  
9 the very surface of the ice. Then, when sea ice reached ca. 25 cm of ice thickness, strong  
10 solubility changes triggered gas bubble formation, which have favoured CH<sub>4</sub> accumulation in  
11 ice. CH<sub>4</sub> retention in the ice was twice as efficient as that of salt. However, as sea ice  
12 thickened, temperature and brine salinity gradient were no more sufficient to trigger bubble  
13 nucleation, and CH<sub>4</sub> was then trapped in the dissolved state, as salt did. The subsequent  
14 evolution of [CH<sub>4</sub>] in sea ice layers mainly depended on physical processes, as chlorophyll-a  
15 and phosphate concentrations did not support in situ CH<sub>4</sub> production, and as CH<sub>4</sub> oxidation  
16 was likely insignificant. Abrupt changes in [CH<sub>4</sub>] in sea ice occurred when sea ice became  
17 permeable; these were associated with the release of gas bubbles to the atmosphere.  
18 Therefore, the main role of our landfast sea ice in the exchange of CH<sub>4</sub> from seawater to the  
19 atmosphere was its control on the amount of CH<sub>4</sub> that it is able to store in its impermeable  
20 layers and the duration of such storage.

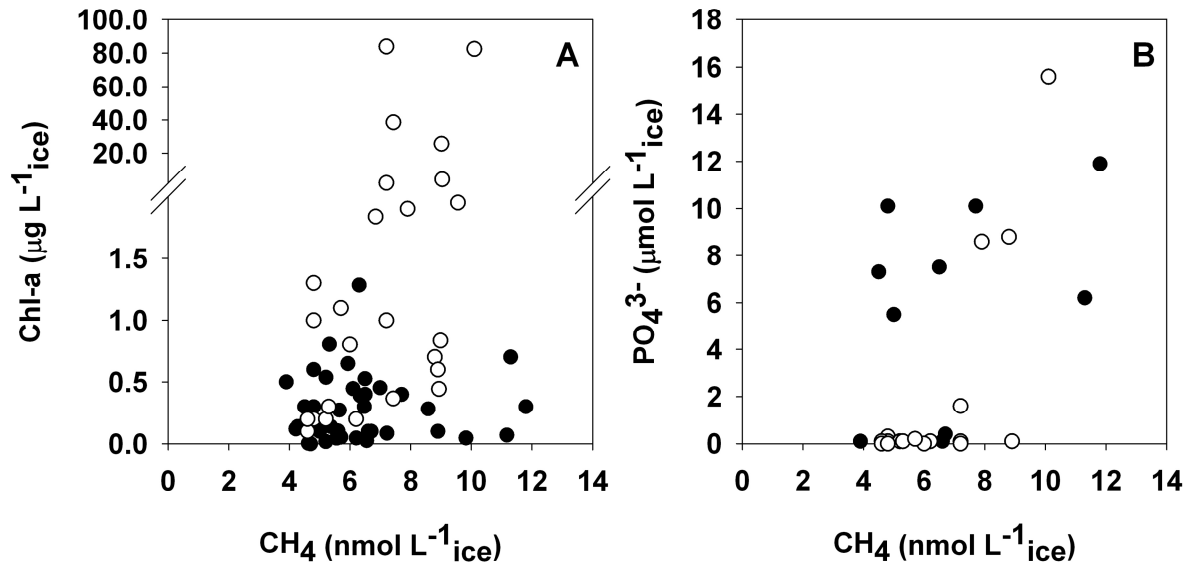
21 Although gas incorporation and sea ice permeability were two dominant factors driving CH<sub>4</sub>  
22 concentrations in sea ice in our study site, the magnitude of these processes may be different  
23 in other polar seas. Indeed, the contribution of the ebullition fluxes of CH<sub>4</sub> from sediment to  
24 the concentration of CH<sub>4</sub> in bulk ice, the transport of CH<sub>4</sub> through the ice, the significance of  
25 physical and biological controls on CH<sub>4</sub> dynamics rely on the nature of the sediment, the  
26 water depth, the physical parameters of the ice and biological activity within the ice, which  
27 may vary depending on the location.

28 In case of a higher mix of physical and biological controls on CH<sub>4</sub> concentrations in bulk ice,  
29 we would recommend to measure: (1) the carbon and hydrogen isotopes of CH<sub>4</sub> in sea ice, as  
30 isotopic fractionation is highly sensitive to biological processes, and (2) the same isotopes in  
31 the sources (e.g., organic matter). Indeed, previous studies have suggested that biogenic CH<sub>4</sub>  
32 within anoxic sediments may have carbon isotopic values as negative as -110 ‰ (Whiticar,

1 1999), in comparison to that formed by CH<sub>4</sub> oxidation (-10 to -24‰ (Damm et al., 2008;  
2 Schubert et al., 2011)), but few of them have considered that the measured isotopic values in  
3 the sediment or in seawater also depend on the isotopic composition of the sources.

4

5 **Appendix A: Relationships between chlorophyll-a and [CH<sub>4</sub>] and between**  
6 **phosphate and [CH<sub>4</sub>] in sea ice**



7

8 A1: Relationships between (A) chlorophyll-a (Chl-a) and methane (CH<sub>4</sub>) concentrations, and  
9 (B) phosphate (PO<sub>4</sub><sup>3-</sup>) and CH<sub>4</sub> concentrations, in sea ice. Open and closed circles indicate  
10 respectively permeable and impermeable ice layers (i.e., brine volume fraction above or  
11 below 5 %). Chl-a and PO<sub>4</sub><sup>3-</sup> data are from Zhou et al. (2013): Chl-a data were available for  
12 all the sampling events that are presented here, while PO<sub>4</sub><sup>3-</sup> were only available for BRW2,  
13 BRW7 and BRW10.

14

15 **Acknowledgements**

16 The authors would like to thank Dr. Hajo Eicken, the rest of the sea ice group of the  
17 Geophysical Institute of the University of Alaska Fairbanks, Tim Papakyriakou, Bernard  
18 Heinesch, Michel Yernaux, Frédéric Brabant, Thomas Goossens, Noémie Carnat and Rodd  
19 Laing for their help in fieldwork. We are indebted to the Barrow Arctic Science Consortium  
20 and the North Slope Borough for their logistical support. We also thank Saïda El Amri and

1 Arnaud Rottier for their efficient help in laboratory work, Ceri Middleton for language help,  
2 Célia Sapart and Neige Egmont for their comments. Our gratitude also goes to the three  
3 anonymous reviewers as their comments have greatly improved the quality of the manuscript.  
4 This research was supported by the F.R.S-FNRS (contract 2.4584.09), the National Science  
5 Foundation (project OPP-0632398 (SIZONet)), the University of Alaska Fairbanks and the  
6 Belgian Science Policy (contract SD/CA/03A), the NCE ArcticNet and National Science and  
7 Engineering Research Council (NSERC). NXG received a PhD grant from F.R.S.-FRIA and  
8 acknowledges the Canada Excellence Research Chair Program and the Arctic Science  
9 Partnership (ASP). JZ is a research fellow of F.R.S.-FNRS, and BD is a research associate of  
10 F.R.S.-FNRS. This is MARE contribution no. XXX.

11



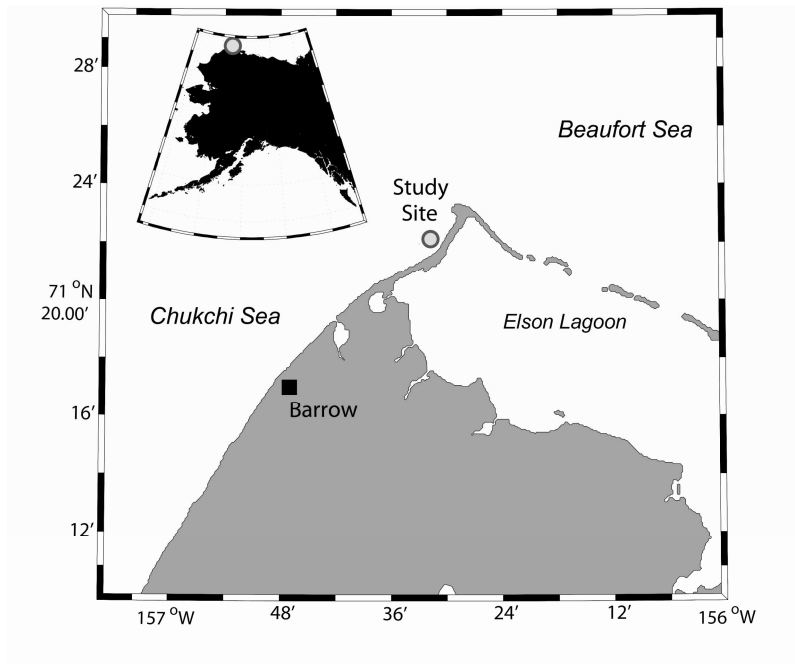
## 1 **References**

- 2 Abril, G. and Iversen, N.: Methane dynamics in a shallow non-tidal estuary (Randers Fjord,  
3 Denmark), *Mar Ecol-Prog Ser*, 230, 171-181, 2002.
- 4 Bange, H. W., Bartell, U. H., Rapsomanikis, S., and Andreae, M. O.: Methane in the Baltic  
5 and North Seas and a Reassessment of the Marine Emissions of Methane, *Global*  
6 *Biogeochem. Cycles*, 8, 465-480, 1994.
- 7 Bates, T. S., Kelly, K. C., Johnson, J. E., and Gammon, R. H.: A reevaluation of the open  
8 ocean source of methane to the atmosphere, *Journal of Geophysical Research*, 101, 6953-  
9 6961, 1996.
- 10 Borges, A. V. and Abril, G.: 5.04 - Carbon Dioxide and Methane Dynamics in Estuaries. In:  
11 *Treatise on Estuarine and Coastal Science*, Editors-in-Chief: Eric, W. and Donald, M. (Eds.),  
12 Academic Press, Waltham, 2011.
- 13 Cox, G. F. N. and Weeks, W. F.: Equations for determining the gas and brine volumes in sea-  
14 ice samples, *J Glaciol*, 29, 306-316, 1983.
- 15 Damm, E., Helmke, E., Thoms, S., Schauer, U., Nöthig, E., Bakker, K., and Kiene, R. P.:  
16 Methane production in aerobic oligotrophic surface water in the central Arctic Ocean  
17 *Biogeosciences*, 7, 1099-1108, 2010.
- 18 Damm, E., Kiene, R. P., Schwarz, J., Falck, E., and Dieckmann, G.: Methane cycling in  
19 Arctic shelf water and its relationship with phytoplankton biomass and DMSP, *Mar Chem*,  
20 109, 45-59, 2008.
- 21 Damm, E., Schauer, U., Rudels, B., and Haas, C.: Excess of bottom-released methane in an  
22 Arctic shelf sea polynya in winter, *Cont. Shelf Res.*, 27, 1692-1701, 2007.
- 23 Florez-Leiva, L., Damm, E., and Farías, L.: Methane production induced by dimethylsulfide  
24 in surface water of an upwelling ecosystem, *Prog Oceanogr*, doi:  
25 <http://dx.doi.org/10.1016/j.pocean.2013.03.005>, 2013. 2013.
- 26 Geilfus, N. X., Carnat, G., Dieckmann, G. S., Halden, N., Nehrke, G., Papakyriakou, T.,  
27 Tison, J. L., and Delille, B.: First estimates of the contribution of CaCO<sub>3</sub> precipitation to the  
28 release of CO<sub>2</sub> to the atmosphere during young sea ice growth, *Journal of Geophysical*  
29 *Research: Oceans*, 118, 244-255, 2013.
- 30 Geilfus, N. X., Carnat, G., Papakyriakou, T., Tison, J. L., Else, B., Thomas, H., Shadwick, E.,  
31 and Delille, B.: Dynamics of pCO<sub>2</sub> and related air-ice CO<sub>2</sub> fluxes in the Arctic coastal zone  
32 (Amundsen Gulf, Beaufort Sea), *Journal of Geophysical Research C: Oceans*, 117, 2012.
- 33 Gleitz, M., v.d.Loeff, M. R., Thomas, D. N., Dieckmann, G. S., and Millero, F. J.:  
34 Comparison of summer and winter in organic carbon, oxygen and nutrient concentrations in  
35 Antarctic sea ice brine, *Mar Chem*, 51, 81-91, 1995.
- 36 Golden, K. M., Ackley, S. F., and Lytle, V. I.: The percolation phase transition in sea ice,  
37 *Science*, 282, 2238-2241, 1998.
- 38 He, X., Sun, L., Xie, Z., Huang, W., Long, N., Li, Z., and Xing, G.: Sea ice in the Arctic  
39 Ocean: Role of shielding and consumption of methane, *Atmos Environ*, 67, 8-13, 2013.
- 40 Judd, A. G.: Natural seabed gas seeps as sources of atmospheric methane, *Environmental*  
41 *Geology*, 46, 988-996, 2004.

- 1 Karl, D. M., Beversdorf, L., Bjorkman, K. M., Church, M. J., Martinez, A., and DeLong, E.  
2 F.: Aerobic production of methane in the sea, *Nat Geosci*, 1, 473-478, 2008.
- 3 Keller, M. and Stallard, R. F.: Methane emission by bubbling from Gatun Lake, Panama,  
4 *Journal of Geophysical Research*, 99, 8307-8319, 1994.
- 5 Kirschke, S., Bousquet, P., Ciais, P., Saunois, M., Canadell, J. G., Dlugokencky, E. J.,  
6 Bergamaschi, P., Bergmann, D., Blake, D. R., Bruhwiler, L., Cameron-Smith, P., Castaldi, S.,  
7 Chevallier, F., Feng, L., Fraser, A., Heimann, M., Hodson, E. L., Houweling, S., Josse, B.,  
8 Fraser, P. J., Krummel, P. B., Lamarque, J.-F., Langenfelds, R. L., Le Quere, C., Naik, V.,  
9 O'Doherty, S., Palmer, P. I., Pison, I., Plummer, D., Poulter, B., Prinn, R. G., Rigby, M.,  
10 Ringeval, B., Santini, M., Schmidt, M., Shindell, D. T., Simpson, I. J., Spahni, R., Steele, L.  
11 P., Strode, S. A., Sudo, K., Szopa, S., van der Werf, G. R., Voulgarakis, A., van Weele, M.,  
12 Weiss, R. F., Williams, J. E., and Zeng, G.: Three decades of global methane sources and  
13 sinks, *Nature Geosci*, 6, 813-823, 2013.
- 14 Kitidis, V., Upstill-Goddard, R. C., and Anderson, L. G.: Methane and nitrous oxide in  
15 surface water along the North-West Passage, Arctic Ocean, *Mar Chem*, 121, 80-86, 2010.
- 16 Kort, E. A., Wofsy, S. C., Daube, B. C., Diao, M., Elkins, J. W., Gao, R. S., Hints, E. J.,  
17 Hurst, D. F., Jimenez, R., Moore, F. L., Spackman, J. R., and Zondlo, M. A.: Atmospheric  
18 observations of Arctic Ocean methane emissions up to 82[deg] north, *Nature Geosci*, 5, 318-  
19 321, 2012.
- 20 Kvenvolden, K., Lilley, M. D., and Lorenson, T. D.: The Beaufort Sea Continental Shelf as a  
21 seasonal source of atmospheric methane, *Geophys. Res. Lett.*, 20, 2459-2462, 1993.
- 22 Lawrence, D. M., Slater, A. G., Tomas, R. A., Holland, M. M., and Deser, C.: Accelerated  
23 Arctic land warming and permafrost degradation during rapid sea ice loss, *Geophys Res Lett*,  
24 35, 2008.
- 25 Loose, B., McGillis, W. R., Schlosser, P., Perovich, D., and Takahashi, T.: Effects of  
26 freezing, growth, and ice cover on gas transport processes in laboratory seawater experiments,  
27 *Geophys Res Lett*, 36, 2009.
- 28 Lorenson, T. D. and Kvenvolden, K. A.: Methane in coastal seawater, sea ice and bottom  
29 sediments, Beaufort Sea, Alaska: U.S. Geological Survey Open-File Report 95-70, US  
30 Geological Survey, Menlo Park, CA, 1995.
- 31 McGinnis, D. F., Greinert, J., Artemov, Y., Beaubien, S. E., and Wüest, A.: Fate of rising  
32 methane bubbles in stratified waters: How much methane reaches the atmosphere?, *Journal of*  
33 *Geophysical Research*, 111, 2006.
- 34 Myhre, G., D. Shindell, F.-M. Bréon, W. Collins, J. Fuglestedt, J. Huang, D. Koch, J.-F.  
35 Lamarque, D. Lee, B. Mendoza, T. Nakajima, A. Robock, G. Stephens, T. Takemura, and  
36 Zhang, H.: *Anthropogenic and Natural Radiative Forcing*, Cambridge University Press,  
37 Cambridge, United Kingdom and New York, NY, USA, 2013.
- 38 Nomura, D., Eicken, H., Gradinger, R., and Shirasawa, K.: Rapid Physically driven invasion  
39 of the air-sea ice CO<sub>2</sub> flux in the seasonal landfast ice off Barrow, Alaska after onset of  
40 surface melt, *Cont. Shelf Res.*, 30, 1998-2004, 2010.
- 41 Nomura, D., Yoshikawa-Inoue, H., and Toyota, T.: The effect of sea-ice growth on air-sea  
42 CO<sub>2</sub> flux in a tank experiment, *Tellus Series B Chemical and Physical Meteorology*, 58, 418-  
43 426, 2006.

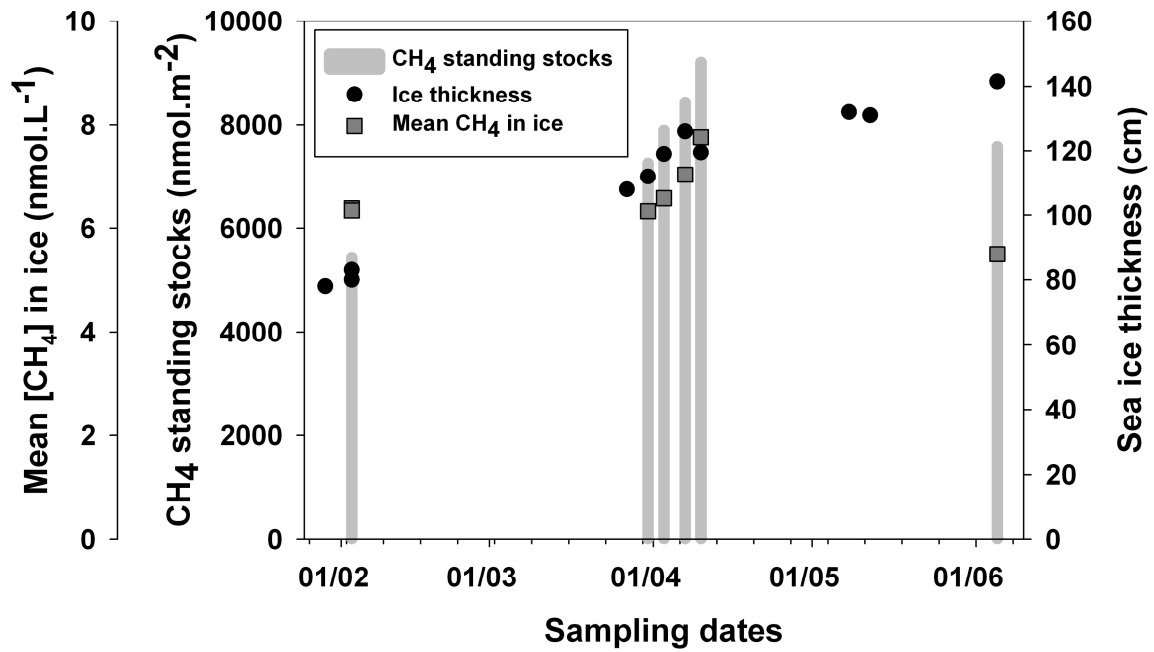
- 1 Notz, D. and Worster, M. G.: Desalination processes of sea ice revisited, *Journal of*  
2 *Geophysical Research*, 114, 2009.
- 3 O'Connor, F. M., Boucher, O., Gedney, N., Jones, C. D., Folberth, G. A., Coppel, R.,  
4 Friedlingstein, P., Collins, W. J., Chappellaz, J., Ridley, J., and Johnson, C. E.: Possible role  
5 of wetlands, permafrost, and methane hydrates in the methane cycle under future climate  
6 change: A review, *Rev Geophys*, 48, RG4005, 2010.
- 7 Papadimitriou, S., Thomas, D. N., Kennedy, H., Haas, C., Kuosa, H., Krell, A., and  
8 Dieckmann, G. S.: Biogeochemical composition of natural sea ice brines from the Weddell  
9 Sea during early austral summer, *Limnol Oceanogr*, 52, 1809-1823, 2007.
- 10 Petrich, C. and Eicken, H.: Growth, Structure and Properties of Sea Ice. In: *Sea ice*, Thomas,  
11 D. N. and Dieckmann, G. S. (Eds.), Blackwell Publishing Ltd, UK, 2010.
- 12 Raynaud, D., Delmas, R., Ascencio, J. M., and Legrand, M.: Gas extraction from polar ice  
13 cores: a critical issue for studying the evolution of atmospheric CO<sub>2</sub> and ice-sheet surface  
14 elevation, *Ann Glaciol*, 3, 265-268, 1982.
- 15 Reagan, M. T. and Moridis, G. T.: Dynamic response of oceanic hydrate deposits to ocean  
16 temperature change, *Journal of Geophysical Research*, 113, 2008.
- 17 Romanovskii, N. N., Hubberten, H. W., Gavrilov, A. V., Tumskey, V. E., Tipenko, G. S.,  
18 Grigoriev, M. N., and Siegert, C.: Thermokarst and land-ocean interactions, Laptev Sea  
19 Region, Russia, *Permafrost Periglac*, 11, 137-152, 2000.
- 20 Savvichev, A. S., Rusanov, I. I., Yusupov, S. K., Pimenov, N. V., Lein, A. Y., and Ivanov, M.  
21 V.: The biogeochemical cycle of methane in the coastal zone and littoral of the Kandalaksha  
22 Bay of the White Sea, *Microbiology+*, 73, 457-468, 2004.
- 23 Schubert, C. J., Vazquez, F., Lösekann-Behrens, T., Knittel, K., Tonolla, M., and Boetius, A.:  
24 Evidence for anaerobic oxidation of methane in sediments of a freshwater system (Lago di  
25 Cadagno), *FEMS Microbiology Ecology*, 76, 26-38, 2011.
- 26 Shakhova, N., Semiletov, I., and Panteleev, G.: The distribution of methane on the Siberian  
27 Arctic shelves: Implications for the marine methane cycle, *Geophys. Res. Lett.*, 32, 2005.
- 28 Shakhova, N., Semiletov, I., Salyuk, A., Yusupov, V., Kosmach, D., and Gustafsson, O.:  
29 Extensive Methane Venting to the Atmosphere from Sediments of the East Siberian Arctic  
30 Shelf, *Science*, 327, 1246-1250, 2010.
- 31 Skoog, D. A., West, D. M., and Holler, F. J.: *Chimie analytique*, De Boeck Université, Paris,  
32 Bruxelles, 1997.
- 33 Untersteiner, N.: Natural desalinisation and equilibrium salinity profile of perennial sea ice,  
34 *Journal of Geophysical Research*, 73, 1251-1257, 1968.
- 35 Upstill-Goddard, R. C., Barnes, J., Frost, T., Punshon, S., and Owens, N. J. P.: Methane in the  
36 southern North Sea: Low-salinity inputs, estuarine removal, and atmospheric flux, *Global*  
37 *Biogeochem. Cycles*, 14, 1205-1217, 2000.
- 38 Weeks, W. F.: *On sea ice*, University of Alaska Press, Fairbanks, Alaska, 2010.
- 39 Westbrook, G. K., Thatcher, K. E., Rohling, E. J., Piotrowski, A. M., Pälike, H., Osborne, A.  
40 H., Nisbet, E. G., Minshull, T. A., Lanoisellé, M., James, R. H., Hühnerbach, V., Green, D.,  
41 Fisher, R. E., Crocker, A. J., Chabert, A., Bolton, C., Beszczynska-Möller, A., Berndt, C., and  
42 Aquilina, A.: Escape of methane gas from the seabed along the West Spitsbergen continental  
43 margin, *Geophys Res Lett*, 36, L15608, 2009.

- 1 Whiticar, M. J.: Carbon and hydrogen isotope systematics of bacterial formation and  
2 oxidation of methane, *Chem Geol*, 161, 291-314, 1999.
- 3 Wiesenburg, D. A. and Guinasso, N. L.: Equilibrium solubilities of methane, carbon  
4 monoxide and hydrogen in water and sea water, *J. Chem. Eng. Data*, 24, 356-360, 1979.
- 5 Yamamoto, S., Alcauskas, J. B., and Crozier, T. E.: Solubility of methane in distilled water  
6 and seawater, *Journal of Chemical & Engineering Data*, 21, 78-80, 1976.
- 7 Zeikus, J. G. and Winfrey, M. R.: Temperature limitation of methanogenesis in aquatic  
8 sediments, *Appl Environ Microb*, 31, 99-107, 1976.
- 9 Zhou, J., Delille, B., Eicken, H., Vancoppenolle, M., Brabant, F., Carnat, G., Geilfus, N.-X.,  
10 Papakyriakou, T., Heinesch, B., and Tison, J.-L.: Physical and biogeochemical properties in  
11 landfast sea ice (Barrow, Alaska): Insights on brine and gas dynamics across seasons, *Journal*  
12 *of Geophysical Research: Oceans*, 118, 3172-3189, 2013.
- 13 Zindler, C., Bracher, A., Marandino, C. A., Taylor, B., Torrecilla, E., Kock, A., and Bange, H.  
14 W.: Sulphur compounds, methane, and phytoplankton: interactions along a north-south transit  
15 in the western Pacific Ocean, *Biogeosciences Discuss.*, 9, 15011-15049, 2012.
- 16
- 17



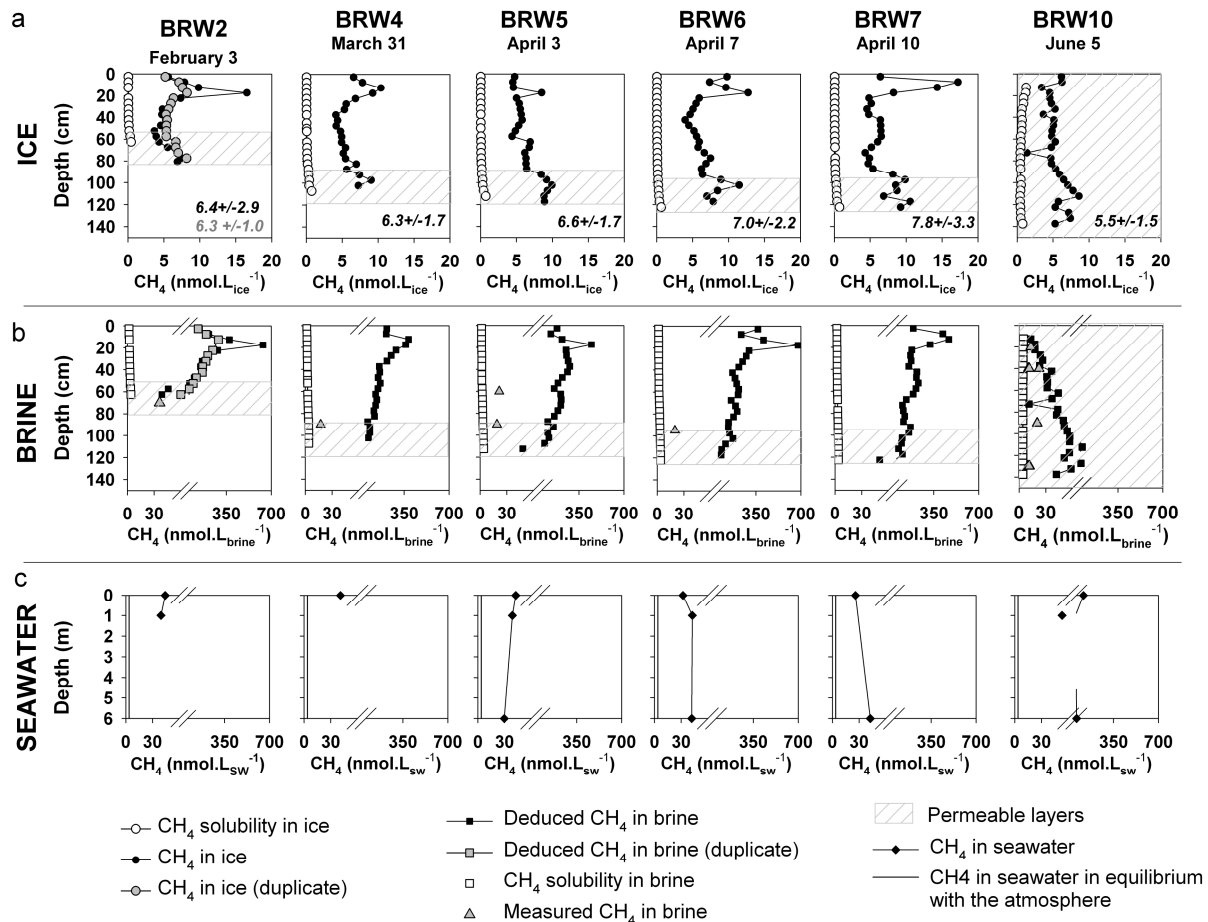
1

2 Figure 1. The study site. North of Barrow, Alaska, US.



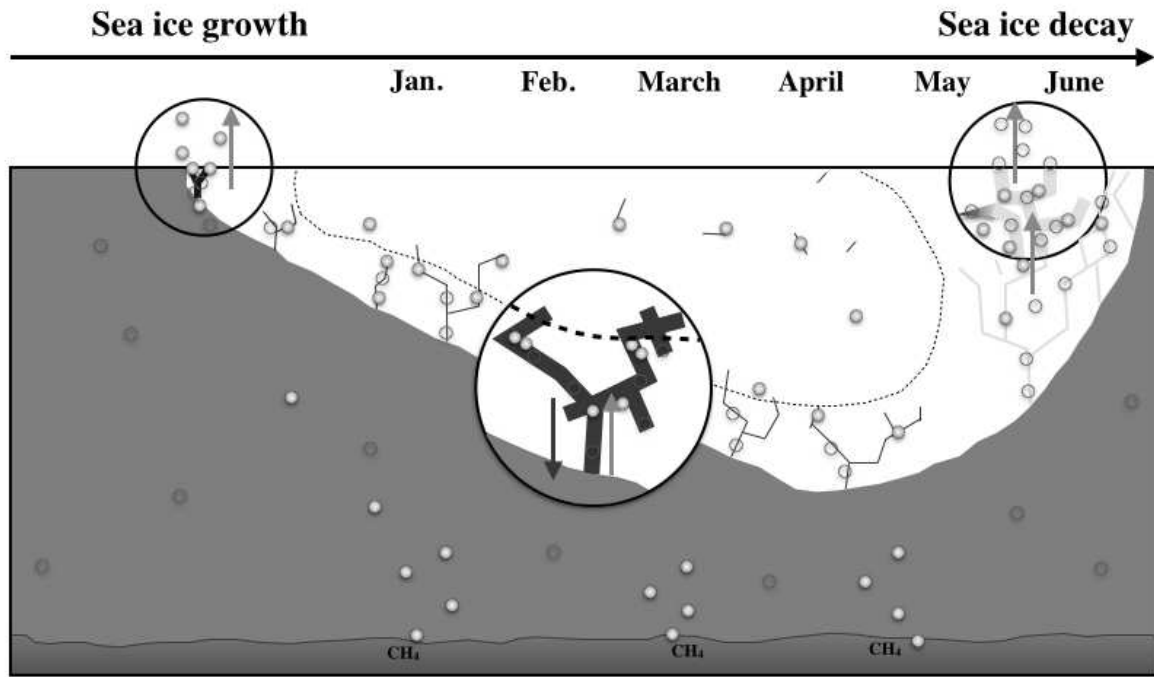
1

2 Figure 2. CH<sub>4</sub> standing stocks for selected samplings events (vertical bars, from left to right,  
 3 BRW2, BRW4, BRW5, BRW6, BRW7 and BRW10) in parallel with mean [CH<sub>4</sub>] in sea ice  
 4 and sea ice thickness.



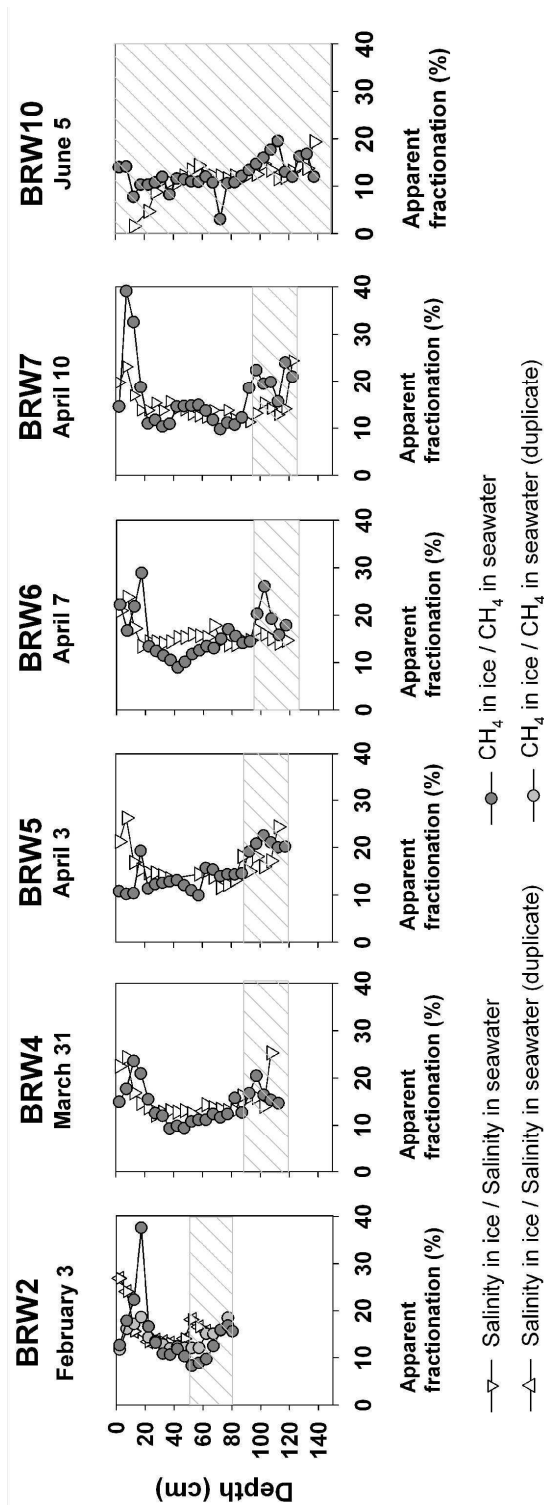
1  
 2 Figure 3. Evolution of CH<sub>4</sub> concentration in (a) bulk ice, (b) brine and (c) seawater (black  
 3 dots, squares and diamonds respectively), compared to CH<sub>4</sub> solubility in ice, brine and  
 4 seawater that is in equilibrium with the atmosphere (white dots, white squares and black  
 5 straight lines respectively). Grey dots and grey squares are measurements made on duplicate  
 6 samples of BRW2. Grey triangles in (b) are CH<sub>4</sub> measurements in brine sackholes. The break  
 7 in the x axes of (b) and (c) is set at 60 nmol L. Dashed areas are permeable layers (i.e. layers  
 8 with brine volume fraction above 5%)

9  
 10  
 11  
 12  
 13



1  
 2 Figure 4. Schematic figure of CH<sub>4</sub> release and incorporation in sea ice. Sizes are intentionally  
 3 disproportionate to better highlight processes. The area above the dotted line represents the  
 4 impermeable layers. The small filled and empty circles represent CH<sub>4</sub> in gas bubbles and in  
 5 dissolved state respectively. Upward grey arrows indicate the upward transport of gas bubbles  
 6 due to their buoyancy, while downward blue arrows indicate the removal of dissolved gas  
 7 through brine drainage. Large black circles zoom on particular processes described in the text  
 8 (Sect. 4.2): gas exchanges at the beginning of ice growth, preferential gas accumulation under  
 9 the impermeable layers and gas bubble escape during ice decay. Dark blue, light blue and  
 10 cyan strokes in ice represent brine channels with high, moderate or low salinity respectively.





1

2 Figure 5. Comparison between the apparent fractionation of salinity in ice (the ratio between  
 3 ice salinity and the seawater salinity (32)) and the apparent fractionation of CH<sub>4</sub> (the ratio  
 4 between CH<sub>4</sub> in ice and CH<sub>4</sub> in seawater (44 nmol L<sup>-1</sup><sub>sw</sub>)). The seawater salinity and CH<sub>4</sub> in  
 5 seawater that are chosen as references were the values obtained from BRW2. Dashed areas  
 6 are permeable layers (i.e. layers with brine volume fraction above 5%).